Disentangling Catalytic Activity at Terrace and Step Sites on Selectively Ru-Modified Well-Ordered Pt Surfaces Probed by CO Electro-oxidation

Manuel J. S. Farias[1,*], William Cheuquepán[2], Giuseppe A. Camara[1], Juan M. Feliu[2]

[1]*Instituto de Química, Universidade Federal de Mato Grosso do Sul, C.P. 549, 79070–900, Campo Grande, Brazil*

[2]*Instituto de Electroquímica, Universidad de Alicante Ap. 99, E–03080, Alicante, Spain*

Abstract

In heterogeneous (electro)catalysis, the overall catalytic output results from responses of surface sites with different catalytic activities, and their discrimination in terms of what specific site is responsible for a given activity is not an easy task. Here, we use the electro-oxidation of CO as a probe reaction to access the catalytic activity of different sites on high Miller index stepped Pt surfaces with their {110} steps selectively modified by Ru at different coverage. Data from *in situ* FTIR spectroscopy and cyclic voltammetry evidence that Ru deposited on {110} steps modifies the surface in a non-trivial way, only favoring the electrocatalytic oxidation of CO over {111} terraces. Moreover, these {111} terraces become catalytically active throughout a large potential window. On the other hand, after the deposition of Ru on {110} steps, the partial oxidation of a CO adlayer (by stripping voltammetry and *in situ* FTIR potential steps) show that those {110} steps that remain free of Ru seem to be not influenced by the presence of this metal. As a result, the remaining CO adlayer is oxidized on these Ru-free {110} steps at potentials identical to those observed in steps of pure stepped Pt surfaces (in absence of Ru). Firstly, these

findings suggest that CO_{ads} behaves as a motionless species during its oxidation. Secondly, they evidence that the impact caused by the presence of Ru in the catalytic activity of Pt(s)-[(*n*-1)(111)×(110)] stepped surfaces depends on the crystallographic orientation of Pt sites. These results help us to shed new light about the role of Ru in the mechanism of oxidation of CO and allow a deeper understanding regarding the CO tolerance in Pt-Ru catalysts.

Keywords: Electrocatalysis, Ru-modified Pt(*hkl*) surfaces, bifunctional mechanism, activity of step sites, CO oxidation, CO surface diffusion.

*Corresponding Author:

manueljsfarias@gmail.com; Phone:+55 67 3345 3596 (M.J.S.F.).

1. Introduction

The electro-oxidation of CO on pure Pt and Pt-based catalysts is a prototypical reaction widely studied due to its pertinence for both polymer electrolyte and direct alcohol fuel cells.[1,2] In electrocatalysis, two metallic surfaces based on combinations of Pt and Ru are still recognized to be promising catalysts for both fuel cells.[3,4] From an historical viewpoint, the deep impact coming from Ru in electrocatalysis of methanol electro-oxidation on Pt-Ru electrodes was reported in a review by Bockris and Wroblowa more than fifty years ago.[5] This subject has received renewed attention over the years, but the elucidation of the synergetic effect existent in Pt-Ru (and Pt in combination with other metals) to explain its catalytic enhancements, for instance, for oxidation of hydrogen poisoned by CO, is not exactly clear.[6] The understanding on the underlying mechanism in the catalytic activity enhancement of Pt by Ru for reactions involving CO in any step pathway might shed light on the opportunity to design efficient catalysts for fuel cells operating with H_2 containing traces of CO as impurity,[7] so that models have been developed to explain the synergism between these metals.

Methanol dissociatively adsorbs on Pt likely originating HCO_{ads} species,[8,9] whose oxidation to CO_2 requires oxygen from water molecules. Based on this proposition, Watanabe and Motoo [10] rationalized the superior catalytic performance of Pt-Ru in terms of the intrinsic Ru ability to promote the water oxidation step ($H_2O \rightleftarrows OH_{ads} + H^+ + e^-$) at low potentials, something that, according to this proposition, Pt is not able to do. According to the so-called bifunctional mechanism at the interface of Pt-Ru each metal in surface should act as responsible for the promotion of different steps in the overall reaction.[10-12] This model has been complemented by an electronic effect (ligand effect).[13,14] Accordingly, Ru produces perturbations in the energy of the surface *d*-band of Pt,[13,15] which can result in modifications on both the strength of Pt-(CO) bond and the

activation energy of reaction, in such a way that on Pt surfaces modified by Ru, Pt-(CO) might be easily oxidized to CO_2 at potentials lower than those required in Pt alone.[14] Besides electronic effects, it is well known that the attachment of foreign atoms to a substrate can also induce changes in the catalytic properties of the substrate, once different equilibrium positions are attained due to strains in lattice constant provoked by these foreign atoms,[16-18] in which both electronic and strain effects are expected to operate simultaneously.[19] The combined action of bifunctional mechanism and electronic effect has been proposed to explain the role of Pt-Ru during CO electro-oxidation,[13] but the bifunctional mechanism is still the predominant model to explain the behavior of such systems.[1,11,12,20-22]

The bifunctional mechanism requires that during CO electro-oxidation the limiting step reaction at low overpotentials is a bimolecular collision between neighboring Pt_κ-(CO) and an activated Ru_γ-(H_2O) species at a threshold potential via a Langmuir-Hinshelwood mechanism, being the formation of the last species promoted on Ru domains. For CO oxidation on a Pt-Ru electrode, it means that Ru domains must act as centers for nucleation of oxygen-containing species, and the occurrence of the bifunctional mechanism requires CO_{ads} diffusion from Pt domains to active Pt sites near Ru sites. Specifically regarding a CO stripping experiment on Pt-Ru surfaces (in which there is no external supply of CO to the surface), in the potential window of CO oxidation, it would be expected that the supply of CO_{ads} to the "active sites" be secured via CO_{ads} diffusion from any Pt sites to those in the Ru surroundings. Conversely, multiple CO stripping peaks would be expected during a voltammetric stripping of CO. In this sense, in absence of anion adsorption in acid solution, the overall CO electro-oxidation at the perimeter of Pt and Ru domains at "lower potentials" should be formally written as:[22-24]

$$Pt_\kappa\text{-}(CO) + Ru_\gamma\text{-}(H_2O) \rightarrow CO_2 + \kappa Pt + \gamma Ru + 2H^+ + 2e^- \quad (1)$$

also at "lower potentials" on Ru domains, the overall reaction is:[23]

$$Ru_{\propto}\text{-}(CO) + Ru_{\gamma}\text{-}(H_2O) \rightarrow CO_2 + (\propto + \gamma)Ru + 2H^+ + 2e^- \quad (2)$$

On the other hand, no matter if CO is adsorbed on step or terrace sites, the oxidation of CO_{ads} on Pt sites far from Ru_{γ}-(H_2O) has been conceived to occur only at "higher" electrode potentials,[23,24] which in such case would be the oxidation of CO on {111} terraces (denoted as Pt_T). Under this condition, the overall reaction should be formally written as:[23,24]

$$Pt_T\text{-}(CO) + Pt_T\text{-}(H_2O) \rightarrow CO_2 + 2Pt_T + 2H^+ + 2e^- \quad (3)$$

Experiments in order to check all these hypotheses require well-structured catalysts and are still scarce in the literature. Aiming to shed some light on this issue, models in which CO_{ads} diffuses from Pt domains to those sites at the periphery of Ru domains have been claimed,[25] although such hypothesis has never been supported by any experimental evidence. On Ru-modified Pt(111) catalysts, whose surface is characterized by a large number of Ru nano-islands on {111} terraces,[26-28] the {111} Pt domains free of Ru have been traditionally claimed to be little active,[23,24] leaving space for a possible interpretation in terms of catalysis promoted via electronic effects induced by Ru on Pt sites, even those far from Ru domains. Moreover, by employing Ru-modified Pt(111) or Ru-modified Pt nanoparticles, besides the restrict CO mobility, the existence of well-defined zones (rich either in Pt or Ru) in such electrodes has been placed at the core of the general framework to explain the origins of the peaks multiplicity in CO stripping voltammetry.[24,25] Hence, multiple peaks might occur in one of the following situations: (*i*) slow CO diffusion from Pt domains to the perimeter of the Ru islands, due unfavorable binding energy;[29] (*ii*) strong adsorbed sulfate hindering CO_{ads} mobility from Pt sites to the periphery of Ru domains;[24] (*iii*) OH_{ads} acting as a barrier for the diffusion of CO to highly active sites.[30]

Alternative interpretations concerning the catalytic enhancement of Pt-Ru have appeared in current literature. By careful correlation between surface structure of Pt deposited on Ru(0001) crystals and its resulting catalytic activity, a potential induced surface restructuring has been pointed out to play a dominant role in the high catalytic activity of those catalysts to the oxidation of bulk CO at lower potentials.[31,32] Moreover, it was also concluded that at low potentials (~0.6 *vs.* RHE/V), Ru(0001) terraces are more active for CO oxidation than the inter-metallic boundary of RuPt, in which the traditional bifunctional mechanism apparently fails.[32] In addition, Chen and Tong[33] recently revised the bifunctional mechanism for methanol oxidation on PtRu electrodes. The authors concluded that the presence of CO on Pt sites in intermetallic boundaries is "irrelevant" for the catalytic enhancement of methanol oxidation at low potentials.[33] According to the authors, a reaction pathway involving adsorbed formate (which decomposes to CO_2) arises at intermetallic PtRu boundaries.[33]

Aiming electrocatalytic applications, the electrodeposition of metals [$M_{(aq)}^{z+} + S_{(s)} + ze^- \rightarrow M/S_{(s)}$] is a widely studied field for the fabrication of bimetallic and multi-metallic materials resulting in different surface structures.[34-37] These structures usually exhibit catalytic activities superior than the individual metals. In many cases, *in situ* STM (Scanning Tunneling Microscopy) studies shown that the growth of new structures (for instance, one-dimension chains and two-dimension ad-islands) on a base substrate is strongly influenced by the presence of sites with low coordination number (steps, defects, kinks and so on), on which metal deposition starts.[38,39] In a previous study, by using underpotential deposition, it has been shown that it is possible to decorate only the steps [having either (110) or (100) symmetry] of Pt high Miller index surfaces with Ru, keeping (111) Pt terraces completely free.[40-42] Compared to pure Pt, the oxidation of CO on these modified surfaces is deeply affected. Namely, the presence of Ru at Pt steps reduces

greatly the onset potential for this reaction, but the kind of sites which have their catalytic activities affected by Ru hitherto has not been elucidated yet. Additionally, for stepped Pt surfaces with similar (111) terrace widths, it was found that the electro-oxidation of CO starts at similar potentials, regardless of whether the steps have {110} or {100} symmetry.[41] Although the Ru deposited forms new steps on the surface, a similar onset potential oxidation indicates that the new structure (Ru steps) cancels the original one (Pt steps). To the best of our knowledge, there is neither *in situ* nor *ex situ* STM topographical studies of electrochemically Ru decorated at Pt stepped surfaces. However, recently Carbonio *et al.*[43] published a study of *ex situ* STM under UHV conditions at room temperature for a Pt(332) surface on which Ru ($\theta_{Ru} \simeq 0.34$ ML) was exclusively attached at the rows of step sites by sputtering deposition. For this Ru coverage, it were resolved both 1D chain and 2D dimensional structures formed by Ru only in Pt steps, while for $\theta_{Ru} \simeq 0.94$ ML, a mix including bilayers was observed.[43] Under electrochemical conditions, selectively deposited Ru at steps of stepped Pt surfaces can be successful checked by cyclic voltammetry when the electrode potential is swept around the hydrogen adsorption/desorption region.[41]

Insights about the mechanism of catalytic influence of Ru in Pt-Ru catalysts can be accessed by using Pt(111) vicinal surfaces selectively modified by Ru, especially if the study starts from experiments whose Pt crystal surfaces were selectively modified by Ru at increasing coverage degrees. This experimental strategy allows assessing the impact of Ru in the catalytic activity of different Pt active sites (terraces and steps, free of Ru). However, as stated before, questions about dynamic/mobility of CO on surfaces as well as the assignment of specific sites (and/or domains) which had its catalytic activity affected by Ru (in steps) remains open. This contribution attempts to address these questions. In order to do that, we selectively decorated {110} steps of Pt(111) vicinal

surfaces by electrochemical deposition of Ru at different coverage. *In situ* FTIR (Fourier Transform Infrared) spectroscopy and cyclic voltammetry at well-defined electrodes were employed to follow the electro-oxidation of a full CO adlayer and with this species previously adsorbed only on step sites.

2. Experimental Section

In this study, we have used stepped Pt crystals, namely Pt(554) and Pt(332), with geometric areas ranging between ~3 and ~5 mm^2, as working electrodes. The Pt crystals were prepared following the procedure described by Clavilier *et al.*.[44] These stepped surfaces contain *n* atom-wide (111) terraces periodically broken by monoatomic steps with {110} symmetry. According with Lang-Joyner-Somorjai[45] (LJS model), those Pt(111) vicinal surfaces can be denoted as Pt(s)-[(*n*–1)(111)×(110)]. In addition, this series of stepped surfaces also might be presented as Pt(s)-[*n*(111)×(111)], but for the purpose of describing electrochemical behavior coming from the (111)×(111) junction that is a step, the former notation is more representative [46] since it is assigned as (110) steps. According with LJS model (and using the first notation), individually the two stepped surfaces above can be represented as:

$$\text{Pt(s)-[9(111)×(110)]} \equiv \text{Pt(554)};$$

$$\text{Pt(s)-[5(111)×(110)]} \equiv \text{Pt(332)}.$$

The Pt crystals were flame annealed in a butane/air flame and cooled down in a controlled H_2/Ar atmosphere. Subsequently, the surface of each crystal was protected by a droplet of deoxygenated (H_2/Ar) water, and then it was transferred to the electrochemical cell. A platinized Pt wire was used as a counter electrode and the reference electrode was a reversible hydrogen electrode (RHE), being all the potentials presented in this scale. All experiments were carried out in 0.1 M $HClO_4$ (Merck

suprapur) solution in ultrapure water (Milli-Q 18.2 MΩ cm). To degasing the electrolyte solution, we used Ar (Alpha Gaz^{TM}, N50). For the stripping experiments, CO (Alpha Gaz^{TM}, N47) was injected directly through solution for 5 min (unless otherwise stated) with the electrode potential kept at 0.100 V. Next, non-adsorbed CO was replaced by Ar bubbling into the solution for 20 min (unless otherwise stated).

To selectively decorate the Pt stepped surfaces with Ru, we employ a solution of $RuCl_3 \cdot xH_2O$ (Merck) whose concentration was of about ~1.4×10^{-5} M prepared in ultrapure water. The electrochemical deposition of Ru was carried out during electrode potential swept in the range of 0.060 V - 0.300 V at 0.05 V s^{-1}. The fraction of {110} steps covered by Ru (denoted as $\theta_{\mathrm{Ru}}^{\mathrm{Step}}$) on stepped Pt surfaces was calculated as:

$$\theta_{\mathrm{Ru}}^{\mathrm{Step}} \simeq \frac{Q_{\mathrm{H}}^{\mathrm{S,0}} - Q_{\mathrm{H}}^{\mathrm{S,Ru}}}{Q_{\mathrm{H}}^{\mathrm{S,0}}} \qquad (4)$$

where $Q_{\mathrm{H}}^{\mathrm{S,0}}$ and $Q_{\mathrm{H}}^{\mathrm{S,Ru}}$ refer to the hydrogen desorption charge densities from steps in Pt clean and after the deposition of Ru, respectively.

To remove deposited Ru from Pt surface, the Pt crystal was wet in concentrated nitric acid, and then it was heated in a butane/air flame until the nitric acid “exploded” on the surface. The procedure was repeated about ten times. Then, the Pt crystal was flame annealed and cooled down as described before, and cyclic voltammograms were collected to confirm the complete removal of Ru. Further, to confirm Ru removal a new CO stripping voltammetry was recorded and compared with an identical experiment before any Ru deposition. In all cases, the absence of extra catalytic activity indicated that Ru was completely removed from the Pt surface. Afterwards, further experiments with other Ru coverage were performed.

For *in situ* FTIR experiments, we employed a Nicolet (Model 8700) spectrometer, equipped with a MTC (Mercury-Cadmium-Telluride) detector and cooled down with

liquid N_2. We used a spectro-electrochemical cell with a thin layer configuration [47] formed by pressing the single crystal against a CaF_2 prismatic (60°) window. Spectra were acquired by the co-addition of 200 averaged scans with a resolution of 8 cm^{-1} (the acquisition time of each spectrum was about 90 s), from 0.060 until 0.800 V, at intervals of 50 mV. The resulting spectra are presented in absorbance units, $A = -\log[(R_0 - R_i)/R_0]$ *vs.* υ/cm^{-1}, in which the term R_0 is a single-beam reflectance reference spectrum either at 0.800 V or 0.060 V (specified in section 3.5), while R_i is a single beam reflectance spectrum at a sample potential. According with the notation for A, positive bands (pointing *up*) in spectra mean that species were formed into the thin layer, while negative ones (pointing *down*) refer to species that were consumed or diffused out from the thin layer. All experiments were made by employing a *p*-polarized radiation which allows to detect IR active species both at the electrode surface and dissolved into the thin layer,[47] according to the surface selection rule.[48,49]

Electrode potentials were controlled by using a waveform generator (EG&G PARC 175) together with a potentiostat (Amel 551) and a digital recorder (eDAC ED 401). All the experiments were carried out at room temperature (25 °C).

3. Results

3.1. Electrochemical Characterization of Unmodified and Ru-Modified Pt Crystals

Figure 1 compares cyclic voltammograms of Pt(554) and Pt(332) crystals before and after their selective modifications by Ru electrochemical deposition. This figure includes hard sphere models for these stepped surfaces. In Figures 1A and 1C, the features of the cyclic voltammograms imply that both surfaces were of high-quality oriented and wet in contact with lightly clean solutions. The reversible feature at ~ 0.128 V is due to

hydrogen desorption/adsorption at {110} step sites. Further details about the description of Pt single crystals in electrochemical solution can be consulted in the work of Climent *et al.*.[50]

Panels B and D in Figure 1 show the evolution of the voltammetric profile after Ru deposition on these crystals. In order to achieve Ru deposition, cyclic voltammograms were first recorded in the supporting electrolyte solution at 0.05 V s^{-1} from 0.060 V to 0.300 V in the meniscus configuration. Next, an aliquot of ruthenium chloride solution was added into the electrochemical cell (~1.4×10^{-5} M) while the potential was swept at 0.05 V s^{-1} from 0.060 up to 0.300 V. After reached a certain degree of suppression in hydrogen desorption/adsorption currents by Ru deposition, a single cyclic voltammogram was recorded from 0.060 V up to 0.800 V at the same scan rate to check the complete voltammetric profile (including the double layer region). As can be seen in Figures 1B and 1D, hydrogen desorption/adsorption at {110} steps is the feature affected by Ru deposition. Based on this finding, it is reasonable to affirm that Ru deposits preferentially at the steps, leaving {111} terraces completely free, as previously reported either by electrochemical deposition[41,43] or sputtering deposition under UHV environments.[43] For Pt(554), the original charge density (in absence of Ru, denoted as $\theta_{\mathrm{Ru}}^{\mathrm{Step}} = 0.00$, black line) under the feature peak at ~0.128 V was of about 28.9 μC cm^{-2}. As Ru deposits on Pt steps, the magnitude of this feature gradually decreases. In red the curve, the remaining charge density was of ~18 μC cm^{-2}, which allows us to estimate the fraction of steps covered by Ru as $\theta_{\mathrm{Ru}}^{\mathrm{Step}} \simeq 0.38$. After a further Ru deposition (blue line), the remaining charge density decreases to ~10 μC cm^{-2}, and the fraction of Pt steps covered by Ru was $\theta_{\mathrm{Ru}}^{\mathrm{Step}} \simeq 0.65$. In last case, the profile of electric double layer (from ~0.35 V up to ~0.65 V) appears considerably disrupted, suggesting that adsorbed Ru undergoes oxygen adsorptive reactions.

For Pt(332), the charge density under the peak centered at ~0.128 V was of 49.9 μC cm^{-2} in absence of Ru (θ_{Ru}^{Step} = 0.00 – black line). After Ru deposition, this charge decreases to ~39.1 μC cm^{-2} and 32.3 μC cm^{-2} resulting in θ_{Ru}^{Step} of about 0.22 and 0.35, respectively. On both surfaces, the general trend is the deposition of Ru preferentially at Pt steps. Only after these sites being fully covered, the occupancy of terraces clearly starts (See Figure SI 1).

3.2. Catalytic Activity towards the Electro-Oxidation of CO without Assignment of Active Sites

Figure 2 displays cyclic voltammetries for the CO oxidation on unmodified and Ru-modified stepped Pt surfaces correspondent to that shown in Figure 1. In these experiments, the electrode potential was kept at 0.100 V, and a saturated CO adlayer was formed as described in section 2. After Ar purging, the CO adlayer was oxidized at once by sweeping the electrode potential from 0.060 V to 0.800 V.

For pure Pt(554) (black lines in Figures 2A or 2B), CO oxidation abruptly starts at ~0.72 V and a single oxidation peak appears at ~0.76 V. The exact potential in which CO oxidation starts will be further examined by *in situ* FTIR, which is a better technique for this purpose. In Figure 2 the CO pre-oxidation was prevented by controlling the time for replacing the solution CO by Ar, as discussed in a previous publication.[51] For θ_{Ru}^{Step} of 0.38 and 0.65 in Pt(554) (red and olive lines, respectively), CO oxidation abruptly starts at ~0.55 V and ends at ~0.76 V. This wide potential window ($\Delta E \simeq$ 210 mV) in which CO oxidizes contrasts with the narrow ΔE (~60 mV, from ~0.72 to ~0.78 V – black line) observed for Pt(554) in absence of Ru. Furthermore, the large ΔE for CO oxidation wave for θ_{Ru}^{Step} of 0.38 and 0.65 in Pt(554) consists of three oxidation peaks, assigned as 1, 2,

and 3, respectively: Peak 1 appears at ~0.57 V, followed by peak 2 at ~0.62 V and peak 3 at ~0.71 V. The magnitude of the peaks depends on the Ru coverage at Pt steps, so that, when $\theta_{\mathrm{Ru}}^{\mathrm{Step}} \simeq 1.0$ (blue line in Figures 2A or 2B), peak 1 becomes dominant. It is worth noting that in case of $\theta_{\mathrm{Ru}}^{\mathrm{Step}} \simeq 1.0$, the potential window for CO oxidation is also very narrow, but a small shoulder persists at ~0.7 V, which can be attributed to the predominance of currents from the formation of Ru oxide/hydroxide. Only for qualitative purposes, we have also estimated the global charge (*i.e.*, the uncorrected charge that includes those currents arising from events taking place to restore the double layer region) of the stripping voltammetry. For Ru coverage of 0.38 and 0.65, the uncorrected charges of CO stripping (integrated from 0.300 V to 0.800 V) were ~443 ± 3 μC cm^{-2}; while for $\theta_{\mathrm{Ru}}^{\mathrm{Step}} \simeq 1.0$, the global charge was ~532 ± 15 μC cm^{-2}. In the last case (blue line), the charge of CO oxidation becomes less accurate because there are strong disturbances in the substrate voltammetry (Figure SI 1), coming from the contribution of oxide/hydroxide (the broad shoulder at ~0.70 V) that makes the estimation of the oxidation charge very imprecise.

In case of Pt(332), displayed in Figure 2C or 2D (black line), CO oxidation abruptly starts after ~0.70 V and presents a single peak starting at ~0.73 V that ends at ~0.76 V, meaning a $\Delta E \simeq 60$ mV. However, when the surface is modified by Ru, the CO oxidation starts at ~0.50 V and persists until ~0.75 V, regardless of Ru coverage. For the lower Ru coverage on Pt steps (coverage 0.22 and 0.35), $\Delta E \simeq 250$ mV. Similar to Pt(554), multiple CO peaks also appear in Ru-modified Pt(332) surfaces. The CO oxidation wave also consists of multiple oxidation peaks and peak 1 also becomes more prominent as Ru coverage increased to $\theta_{\mathrm{Ru}}^{\mathrm{Step}} \simeq 1.0$. For $\theta_{\mathrm{Ru}}^{\mathrm{Step}}$ 0.22 and 0.35 the uncorrected charge of CO stripping (0.300 V - 0.800 V) was of 431 ± 6 μC cm^{-2}, while for $\theta_{\mathrm{Ru}}^{\mathrm{Step}} \simeq 1.0$, it was of

~585 μC cm^{-2}. The reasons for the high charge density and higher uncertainty of CO oxidation charge at high Ru coverage are the same already discussed for Pt(554).

Figure 3 compares CO stripping on both Pt(554) and Pt(332) having similar Ru coverage on Pt steps. On Ru-modified Pt(332), the CO oxidation starts abruptly about 50 mV earlier than on Ru-modified Pt(554). The shift in the onset potential for CO oxidation might be attributed to the width of the {111} terraces. This trend was confirmed by us using a Ru-modified Pt(331) (Figure SI 2), on which the potential of CO oxidation was lower than on Pt(554) and on Pt(332). Finally, on both surfaces CO oxidation persists at high potentials (~0.75 V).

3.3. Catalytic Activity Assignment of Terraces and Steps by Voltammetry During the Stripping of a Partial CO Adlayer

Figure 4 shows partial oxidation of a saturated CO adlayer on Ru-modified stepped Pt surfaces. Here, the formation of CO adlayer and elimination of non-adsorbed CO were done as above. However, the upper potentials were controlled to secure that the CO adlayer was oxidized portion by portion, instead of at once. Thus, starting with a complete CO adlayer on Pt(554) modified by $\theta_{\mathrm{Ru}}^{\mathrm{Step}} \simeq 0.38$ (Figure 4A), in the first cycle (red line), the electrode potential was swept up to 0.620 V, and then it was stepped back to 0.100 V, before the re-start of the sweep. At the end of each partial stripping excursion, the electrode potential was always stepped back to 0.100 V. The currents of the second cycle (blue line) show that those sites available for hydrogen desorption after the first cycle were exclusively {111} terraces. Subsequent cycles continue releasing only {111} terrace sites, and only at the 5$^{\mathrm{th}}$ cycle (olive line), Pt step sites become free. Then the CO electro-oxidation peak appears at ~0.72 V. The oxidation peak at ~0.72 V is assigned to the

oxidation of CO_{ads} on the step sites which remained free from Ru (*i.e.*, Ru has never been adsorbed on these particular sites). This figure also displays a voltammetric sweep for the complete CO adlayer oxidation in a single sweep (black line). As can be seen in Figure 4A, contributions of peaks 1 and 2 (as designated in Figure 2) are exclusively due to the CO oxidation over {111} terraces, while peak 3 is due to the CO oxidation on both terraces and steps. It is important to clarify that by cyclic voltammetry we cannot know if the contribution from CO oxidation on Ru sites develops in processes 1, 2 or 3. This issue will be discussed after *in situ* FTIR experiments (and will be addressed in the next section).

The observations done for Ru-modified Pt(554) in Figure 4A can be extrapolated to the CO electro-oxidation on Ru-modified Pt(332) shown in Figure 4B, in which $\theta_{\mathrm{Ru}}^{\mathrm{Step}} \simeq 0.35$. That means that ~65 % of {110} Pt steps were free for CO adsorption without being previously modified by Ru adsorption. As in Figure 4A, at the end of CO adlayer oxidation, the peak of CO oxidation at steps grows only at ~0.72 V (olive line).

3.4. Intrinsic Catalytic Activity at (110) Pt Steps Modified and non-Modified by Ru

First, in this work, we will define *intrinsic catalytic activity* at {110} Pt steps as the catalytic activity toward CO oxidation when {111} terraces were completely free of CO. In this case, it is possible to perform comparisons between potentials required for CO oxidation on pure Pt steps (before Ru adsorption) and those Pt step sites that remain free after the surface being modified by Ru (hereafter designed as "remaining Pt steps"). Thus, in order to record the experiments shown in Figure 5, a CO adlayer was formed on each surface (Ru-modified or not) and then it was voltammetrically stripped from the terraces until CO_{ads} remained only in Pt step sites. Figure 5 compares CO oxidation on Pt steps of

Pt(554) surfaces at two conditions: (1) pure Pt steps, *i.e.*, Pt steps in stepped surfaces that have not being modified by Ru; (2) remaining Pt steps. As can be seen in Figure 5, the potentials in which CO oxidation starts at Pt steps (no matter if it they had or not Ru as neighbor) are essentially identical (~0.66 V). The oxidation develops a peak at ~0.72 V and ends at ~0.76 V for all cases.

From Figure 5 we can see that for pure Pt steps (black line), there are sites free for hydrogen desorption even before CO being oxidized (peak at ~0.13 V), which means that although the CO coverage at pure {110} Pt steps is not complete, the corresponding CO oxidation charge during the stripping was higher (charge over the peak at ~0.72 V). Such apparent discrepancy suggests that the CO_{ads} which persisted until 0.72 V was that adsorbed in the remaining Pt steps, and not the one adsorbed on Ru sites. Such behavior is expected since "pure" Ru is highly catalytic towards CO electro-oxidation.[14]

3.5. Catalytic Activity Assignment of Terraces and Steps by in situ FTIR Spectroscopy

CO electro-oxidation on pure and Ru-modified stepped Pt surfaces was studied by *in situ* FTIR spectroscopy. Figure 6 shows spectra for CO on pure Pt(332). To record this experiment, the electrode potential was kept at 0.100 V and CO was bubbled into the solution for 3 min. Next, non-adsorbed CO was replaced by Ar gas (12 min of purge). Spectra in Figure 6B show wavenumbers ranging from 1750 to 2230 cm^{-1} for a complete CO adlayer. Spectra exhibit two potential-dependent CO bands.[52] For instance, the spectrum at 0.150 V (red line) shows a band at 2064 cm^{-1} attributed to the stretching υ(C-O) mode of linearly bonded CO (denoted as CO^{L}) mainly on {111} terraces; other band appears at ~1828 cm^{-1} attributed to the stretching υ(C-O) mode of bridge-bonded CO (denoted as CO^{B}) on {111} terraces. Both CO bands survive until about 0.60 V (blue

line), after which they disappear due to the oxidation of the CO adlayer. Figure 6A shows the stretch vibration of CO_2 band (2343 cm^{-1}) for various potentials for the same experiment shown in Figure 6B. We note that the formation of CO_2 starts at ~0.50 V.

Figure 6C displays spectra for CO adsorbed only on {110} Pt steps of a Pt(332) surface. In this experiment, the CO adlayer was formed and non-adsorbed CO was eliminated from solution as described before. Then, the CO adsorbed on {111} Pt terraces was voltammetrically eliminated by controlling the upper potential limit, in order to maintain the population of adsorbed CO on Pt steps intact. Spectra in Figure 6C exhibit a single potential-dependent band, which is attributed to CO^L on {110} Pt steps. For instance, at 0.150 V (red line) in Figure 6C, the band appears in 2024 cm^{-1}, *i.e.*, it appears red shifted by about 40 cm^{-1} in comparison to the CO^L band at full coverage shown in Figure 6B. In Figure 6B, the band due to CO at Pt steps was fully invisible due to dipole-dipole coupling effect, in which the phenomenon of intensity transfer occurs to higher frequency at the expenses of lower one.[53,54] Also, the CO^B band is absent in Figure 6C, confirming that {110} Pt steps do not adsorb CO^B, as previously shown.[55] Figure 6B also shows that the potential-dependent frequency for CO^L is not linear in all the potential range. Namely, after 0.50 V, the CO^L frequency decreases and at 0.60 V it becomes identical to the band-frequency for CO^L at Pt steps (Figure 6C, same potential). These spectroscopic findings strongly support the hypothesis that the CO on Pt step sites only oxidizes after all CO molecules on Pt terraces were fully oxidized.

From Figure 6B, the plot of $d\upsilon_{(C\text{-}O)}{}^i/dE$ (Stark tunning effect) from 0.060 V up to 0.450 V (a potential range in which CO does not oxidize to CO_2) is of about 32 cm^{-1} V^{-1} for CO^L, in good agreement with previous results,[56] while for CO^B, $d\upsilon_{(C\text{-}O)}{}^B/dE \simeq 43$ cm^{-1} V^{-1}. For CO on {110} Pt steps (Figure 6C), $d\upsilon_{(C\text{-}O)}{}^L/dE \simeq 51$ cm^{-1} V^{-1}. High $d\upsilon_{(C\text{-}O)}{}^i/dE$

for CO on Pt steps has been reported,[57,58] but the origin of this behavior is not fully understood yet.

Figures 7 and 8 show spectra collected during the electro-oxidation of a complete CO adlayer on a Pt(332) surface with their {110} Pt steps partially modified by Ru at two different coverage. In both cases, a CO adlayer was formed and the subsequent protocol was similar to that already described. In Figure 7B, ($\theta_{\mathrm{Ru}}^{\mathrm{Step}} \simeq 0.58$), spectra show that CO^{L} band frequency has two ranges of potential-dependence, which is similar to the behavior observed in Figure 6B for the same potentials. Figure 7A shows the CO_2 band as a function of the potential. In this case, on Ru-modified Pt(332), the CO_2 formation starts at ~0.40 V, which is about 0.1 V lower than on pure Pt(332) shown in Figure 6A. The band for CO^{B} in Figure 7B is very small. Screening of the IR band of bridge bonded CO has been reported for epitaxial Cu on Pt(111) under ultra-high vacuum environment.[59] It is worth noting in Figure 7B that at the end of CO adlayer oxidation, the CO frequency presents a red shift that is characteristic of CO in Pt steps, resulting in a CO band frequency similar to that shown in Figure 6C for the same potential. This is spectroscopic evidence that the CO adsorbed at remaining Pt steps is oxidized only after all CO on {111} Pt terraces is converted into CO_2, in perfect agreement with data shown in Figure 5. From Figure 7B, the slope of $d\upsilon_{(C\text{-}O)^{L}}/dE$ is ~33 cm^{-1} V^{-1}, which is very similar to that measured for CO on pure Pt(332) shown in Figure 6.

For higher Ru coverage (Figure 8B), *i.e.*, when $\theta_{\mathrm{Ru}}^{\mathrm{Step}} = 1.0$ plus a significant portion of Ru on {111} terraces ($\theta_{\mathrm{Ru}}^{\mathrm{Terrace}} \simeq 0.35$), spectra show three bands attributed to adsorbed CO. For instance, at 0.150 V, the CO^{L} band on {111} Pt terraces appears at 2051 cm^{-1} (downshifted). Meanwhile a new wide band appears at 1984 cm^{-1} ($\Delta\upsilon \simeq$ -85 cm^{-1}), which is characteristic of the vibrational signature of CO^{L} on Ru sites;[14,60] finally, another band

appears at ~1833 cm^{-1} which is attributed to CO^B on Pt sites.[14] The potential at which CO_2 formation starts is ~0.30 V (Figure 8A), that is ~0.1 V lower in comparison to the experiment depicted in Figure 7A.

Only when the total Ru coverage is high, the band at ~1984 cm^{-1} emerges. One reason why this band is not observed in spectra in Figure 7B (low Ru coverage), is likely because bands for both CO^L on Pt and Ru domains are strongly vibrationally coupled. As CO^L on Pt has higher singleton frequency, it predominates[53,54] at the expenses of CO^L on Ru. However, when Ru starts to occupy terraces, the population of CO on Ru sites increases enormously, and the corresponding CO^L band on Ru rises. Worth of notice is that the band intensities for CO^L decrease simultaneously at both Ru and Pt sites (Figure 9). At the end of CO oxidation (spectra at 0.400 V and 0.450 V in Figure 8), bands at ~2036 cm^{-1} and ~2023-2017 cm^{-1} emerge. These bands differ from those obtained either on Pt or on Ru sites. Friedrich *et al.*[61] by using FTIR and Lu *et al.*[62] by using SFG (Sum Frequency Generation) have reported simultaneous decreases in bands of CO both on Pt and Ru sites. For $\theta_{Ru} = 1$ on a Pt(111) in acid media at 0.2 *vs.* RHE/V,[14] a single CO band appeared at 2005 cm^{-1} related to CO^L. But when total $\theta_{Ru} = 0.75$, the authors observed two bands at 2050 cm^{-1} and 2012 cm^{-1}, related to CO^L on Pt and Ru, respectively [14]. Experiments by In Lin *et al.*[14] for Pt(111) with $\theta_{Ru} \simeq 0.2$ also show two CO^L bands, assigned to the adsorption of CO on Pt and Ru sites. However, for $\theta_{Ru} \simeq 0.2$ data of theses authors do not shown, for instance at 0.10 *vs.* RHE/V, any changes in frequency for CO^L at Pt sites compared to the pure Pt(111) crystal. In our case, a similar trend can be seen in Figure 7B when compared to Figure 6B.

From data shown in Figure 8B, the plot of $d\upsilon_{(C\text{-}O)^i}/dE$, from 0.060 V up to 0.300 V, is ~34 cm^{-1} V^{-1} for CO^L on Pt sites and ~38 cm^{-1} V^{-1} for CO^L on Ru ones. In these spectra, CO^B appears ill-defined, so that $d\upsilon_{(C\text{-}O)^B}/dE$ is very imprecise. For a Ru-modified Pt(111),

Friedrich *et al.*[61] found a $d\upsilon_{(C\text{-}O)^L}/dE \simeq 48$ cm^{-1} V^{-1} for CO on Ru sites. In other studies involving Ru-modified Pt(111) surfaces ($\theta_{Ru} \simeq 0.75$), it was found a $d\upsilon_{(C\text{-}O)^L}/dE$ of about 39 cm^{-1} V^{-1} and 43 cm^{-1} V^{-1} for CO on Pt and Ru domains,[14] respectively.

Figure 10 compares spectra for CO_{ads} on different catalysts at two electrode potentials. These spectra were extracted from Figures 6, 7 and 8. In Figure 10A spectra were taken at 0.200 V, *i.e.*, a potential where CO_{ads} is electrochemically stable on this electrode. In Figure 10A (red and black lines), we can see that the CO^L bands on {110} Pt steps and on Ru sites are separated by ~40 cm^{-1}. At 0.500 V (Figure 10B), the band intensity for CO on Ru-modified surfaces ($\theta_{Ru}^{Step} \simeq 0.58$) is very small (blue line), because this electrode is more active than pure Pt at this potential. Another highlight from Figure 10B is the fact that band frequencies (and intensities) in black and blue lines are virtually identical. From this comparison, it is reasonable to assume that the band at 2046 cm^{-1} (blue line – Figure 10B) is due to the linearly bonded CO at the remaining Pt steps. In case of full CO adlayer (dark cyan line), the CO band remains almost intact, due to the low catalytic activity of pure Pt at 0.500 V.

4. General Discussion

4.1. Influence of Ru Decoration

The deposition of Ru from a diluted Ru(III) solution (~1.4×10^{-5} M – low rate of mass transport) on the family of Pt(s)-[(*n*-1)(111)×(110)] stepped surfaces preferentially starts on Pt steps, as can be inferred from the pattern evolution of cyclic voltammetry in hydrogen region (Figures 1B and 1D). This finding is in perfect agreement with data reported earlier.[41,43] Moreover, Ru deposition on the terraces starts only when steps are completely occupied. Similar to the UHV environments,[43] in view of such preferential

Ru deposition, it is reasonable to assume that also under electrochemical conditions, Ru at low coverages on Pt steps forms mainly monoatomic rows along the original crystalline rows of Pt steps. This selective Ru modification of the Pt steps allowed us to successfully study the impact of Ru in the catalytic activity of neighbour {111} terraces and other sites uncovered by Ru. In this respect, it has been evidenced that the most active sites for CO electro-oxidation lie over the terraces in pure Pt(s)-[(*n*-1)(111)×(110)] stepped surfaces (Figure 6), irrespective of the nature of electrolyte solution.[51,55] We found similar trends here, even when the steps are partially modified by Ru (Figures 2, 4 and 7). That is, Ru on the {110} Pt steps deeply modifies the catalytic activity of the {111} Pt terraces, even those away from Ru. However, its influence in the catalytic activity of the {110} remaining uncovered Pt steps is weaker (Figures 4, 5 and 7). Before addressing this subject, it is convenient to discuss the current understanding about the CO electro-oxidation on pure Pt single crystals.

For pure Pt(s)-[(*n*-1)(111)×(110)] stepped surfaces,[51,55] the high catalytic activity toward CO electro-oxidation observed over the {111} Pt terraces has been partially linked to the lower binding of CO on the electronically perturbed terraces provoked by dipole associated to the steps. By employing Pt stepped surfaces, it is well known from surface science studies [63-66] that the adsorption energy of CO at low coordinated sites is larger than on terrace domains. It is likely that such strongly bound CO at the low coordinated sites, at least to some extent, is related to the lower catalytic activity observed for CO (electro)oxidation on step/kink sites. Terraces and steps behave as energetically very different places. According to the Smoluchowski effect,[67,68] the upper part of the steps exhibits a decreased *d*-electron density, while at the bottom of the steps occurs the accumulation of charge density, *i.e.*, at the corrugated surfaces, the dipole moment associated to the steps results in a higher density of unoccupied *d*-states at the top of these

sites. Hence, it is likely that a gradient of energy occurs over {111} terraces, resulting in catalytic consequences, as observed for CO electro-oxidation over these surface domains,[55] in which the low part of the step, *i.e.*, the concave domains of {111} orientation, might be highest catalytic active sites for CO oxidation. When Pt(s)-[(*n*-1)(111)×(110)] stepped surfaces had their steps partially modified by Ru, data in Figures 2 and 4 show that there is a wide potential window along which {111} Pt terraces become more catalytically active for the electro-oxidation of CO. In this case, there is a clear reduction in the onset potential of CO oxidation, but only on the {111} Pt terraces. On other hand, by using two series of Pt(s)-[(*n*-1)(111)×(110)] and Pt(s)-[(*n*)(111)×(100)] stepped surfaces, Chen *et al.*[69] found that the irreversible blockage of their steps either by Te or Bi hinders the catalytic activity of the modified surfaces. Namely, the poisoning effect observed by Chen *et al.*[69] on {111} Pt terraces (the onset potential for CO electro-oxidation shifts to more positive potentials) suggests that when Te or Bi fully block {110} Pt steps, the modified stepped surface presents catalytic activity like a Pt(111) single crystal.[69] In this occasion, those authors assumed that steps/kinks were the most active sites. On the other hand, the modification of steps in Pt stepped surfaces either by ad-atoms as Ru, Mo, or Sn boosts the catalytic activity toward CO electro-oxidation.[40] These results suggest different and non-trivial mechanism played by ad-atoms in modifications of the catalytic activity on {111} Pt terraces in these electrodes. Unfortunately, the structure of these ad-atoms on Pt steps of Pt stepped surfaces is not studied yet.

Here, {111} Pt terraces become catalytically more active once their steps are decorated by Ru simultaneously to the "variation" of site activity when the surface becomes more heterogeneous. That is, the reaction begins to take place into a wide overpotential window ($\Delta\eta$). For instance, for Pt(554) in Figures 2-3, Ru deposition on Pt steps induces a deep change in potential window (ΔE) in which {111} Pt terraces present

high catalytic activity. ΔE increases from 60 mV before Ru deposition (Figure 2A, black line) to 210 mV after Ru deposition (Figure 2A, olive and red lines). Such enlargement in the reaction potential window along which {111} Pt terraces are active to convert CO into CO_2 corresponds to a change in the standard free Gibbs energy of reaction from ~11.6 kJ mol^{-1} to 40.5 kJ mol^{-1}, respectively. At the same time, multiple CO oxidation peaks (whose origin is not fully understood yet) are observed within that potential range of ~210 mV. Furthermore, if Ru at Pt steps affects the catalytic activity over {111} Pt terraces, data in Figure 2 allow us suppose that such effect might depend on the amount of Ru at those steps. Correspondingly, Figure 2 shows that CO oxidation current densities in peak 1 increase as the Ru coverage (on Pt steps) grows. When Pt steps become fully covered by Ru, the oxidation of CO occurs essentially in peak 1 (which turns into a narrow single peak, $\Delta E \simeq 70$ mV, Figure 2, blue line). Such behavior suggests that the catalytic activity grows uniform at long of {111} Pt terraces as the steps are increasingly covered by Ru. Thus, such changing (and tailoring) in the catalytic activity over {111} Pt terraces induced by distant rows of Ru on Pt steps strongly suggests that a long-range effect could act over {111} Pt terraces free of Ru (provoked by either the strain character and/or the ligand effect). Also, Figure 3 (and Figure SI 2) evidence that the extent by which Ru (on steps) affects the catalytic activity of {111} Pt terraces depends on the width of these terraces. Summarizing, the change in catalytic reactivity over {111} Pt terraces seems to be due to an additional change in the magnitude in dipole moment associated to the steps after Ru deposition on Pt steps ($PtRu_{step}$) combined with the {111} Pt terrace width. $PtRu_{step}$ seems to modify the catalytic features of {111} Pt terraces even when they are away from rows of Ru-modified steps. The observations discussed before make clear that the catalytic enhancement of PtRu systems cannot be fully explained based on the traditional bifunctional mechanism, at least for CO stripping, as will be deeper discussed next.

4.2. Mechanistic Considerations

As already highlighted in the introduction, during the stripping of CO, the assumption of the traditional bifunctional mechanism implies in a high CO mobility on the surface from any Pt site to the periphery of Ru islands, since this model assumes the most active sites are located in the PtRu interface. However, experiments depicted in Figures 4 and 7 evidence that {111} Pt terraces are the first sites to be released during the partial oxidation of a CO adlayer, while {110} Pt steps are the last ones. This releasing "hierarchy" evidences that both Ru on Pt steps (forming a $PtRu_{step}$) and remaining Pt steps (*i.e.*, those Pt steps free of Ru) are less catalytically active for the CO oxidation than {111} Pt terraces electronically perturbed by $PtRu_{step}$ (see data in Figures 4, 5 and 7). This result allows to evaluate separately the catalytic activity for CO oxidation in {111} terraces and {110} steps of Pt (those remaining free of Ru) on Ru-modified surfaces. Concerning the catalytic activity of PtRu interfaces to the CO oxidation, by using well-characterized Pt deposited on Ru(0001) crystals, Engstfeld *et al.*[31,32] proposed that the mere presence of Pt in the immediate surroundings of Ru cannot explain the expressive catalytic enhancement for CO bulk oxidation at low potentials. These authors suggested that for Pt deposited on Ru(0001) surfaces, the most active sites likely lie on {0001} Ru terraces rather than at the RuPt interface. Our data shows that for higher Ru coverage (Ru also on Pt terraces), CO on Ru sites as well as CO on {111} Pt terraces are oxidized concurrently (Figure 9). Our data neither rule out nor corroborate the hypothesis that PtRu interfaces are the most catalytic ones, but they convincingly show that $PtRu_{steps}$ and remaining Pt_{steps} are little catalytic active for CO oxidation (Figures 5 and 7), so that, Ru on Pt steps only impacts in the catalytic activity of {111} terraces. Therefore, the influence of Ru in the catalytic role in Pt sites seems to depend on the crystallographic orientation of Pt sites in

Pt(s)-[(*n*-1)(111)×(110)] stepped surfaces. From catalytic viewpoint, according to the Sabatier principle,[70,71] for an optimum catalysis, the binding forces between the catalyst substrate and the reactants (intermediate of reactions) should be intermediate, *i.e*., to achieve high catalytic activity, it should be neither too weak to promote its activation nor too strong to avoid poisoning by them (in order to allow the desorption of products). Based on this principle, for pure Pt stepped surfaces, if water molecules preferentially dissociate in Pt steps unoccupied by CO, it is reasonable to assume that this principle is fewer applicable for the pair $Pt_{\kappa,\ step}$-CO and $Pt_{\gamma,\ step}$-$(H_2O)_{activated}$ at lower potentials, since the formation of CO_2 requires higher over-potentials to take place on these sites (blue line, Figures 6B). Similarly, in case of Ru modified Pt, it seems to be not applicable also for the pair $Pt_{\kappa,\ step}$ -CO and $PtRu_{step}$-$(H_2O)_{activated}$ (olive and blue line, 7B). However, it seems to be better satisfied for the reaction between $Pt_{\gamma,\ terrace}$-CO and $Pt_{\upsilon,\ terrace}$-$(H_2O)_{activated}$, because it would require lower over-potentials (Figures 6B and 7B). Indeed, from solid/gas interface studies,[72-74] it is well known that water adsorption and its dissociation preferentially occur in the upper parts of step edges compared to close-packed domains. In this respect, once the adsorbates strongly adsorb at the steps, this could at least partially explain the higher over-potentials required for the reaction $Pt_{\kappa,\ step}$-CO + $Pt_{\upsilon,\ step}$-(H_2O) → CO_2 + $(\kappa + \upsilon)Pt_{step}$ + $2H^+$ + $2e^-$ compared with those needed to promote the same reaction at the {111} terraces of Pt stepped surfaces, being these latter modified or not by Ru. Therefore, from data in Figures 4, 5 and 7 it is unlikely that a $PtRu_{step}$-$(H_2O)_{activated}$ and a remaining $Pt_{\kappa,\ step}(CO)$ satisfy the Sabatier principle for a Langmuir-Hinshelwood mechanism. Moreover, similarly to the pure Pt(s)-[(*n*-1)(111)×(110)] stepped surfaces previously reported,[51] data in Figure 4 evidence that after partial oxidation of a CO adlayer, on a Ru partially modified Pt step, the sites released in the first voltammetric cycles apparently were not reoccupied by the remaining CO

molecules on surface. This finding means that those molecules behave like motionless species during its oxidation, at least in the time scale of our experiments. Therefore, the sub-adlayer of CO_{ads} seems to behave strictly as a catalytic poison. The apparent absence of CO mobility during its oxidation has a deep implication in the classic bifunctional mean-field mechanism, *i.e.*, the bifunctional mechanism fails to explain the features observed during CO stripping experiments on the catalysts used in this work.

In a previous work, the apparent CO immobility on Ru modified Pt(111) has been attributed to the strong adsorption energy of sulfate/bisulfate.[24] However, we found the same apparent immobility during the oxidation of CO on Pt stepped surfaces in perchloric acid, whose anions are recognized by not being specifically adsorbed[75] or weakly adsorbed on {111} Pt facets.[76] This finding points out that the apparent immobility of CO during its oxidation cannot be explained on the basis of a strong competing adsorption of anions[24] or assuming OH_{ads} as a barrier for CO_{ads} diffusion.[30] Regarding a possible electronic effect from Ru to the Pt sites, Baltruschat *et al.*[36] proposed that the enthalpy of adsorption in the neighborhood of Ru is increased, and this might have implications to supply CO_{ads} via diffusion from any sites to the neighboring of Ru sites, which has been proposed to be unfavorable by DFT calculation by Koper *et al.*.[29] About this topic, in view of both phenomena, *i.e.*, the surface sites hierarchy for CO and because CO_{ads} apparently behaves as a motionless species during its oxidation, we think that data of Figures 4 and 7 are coherent with the existence of a gradient of energy over {111} Pt terraces of Pt stepped surfaces. The remaining question is why oxygen-containing species reach "motionless" CO molecules anywhere on the {111} Pt terraces. On this matter, Davies *et al.*[24] proposed a spillover of activated oxygen containing species from Ru sites to CO_{ads} at any Pt sites, instead of water activation on those disturbed Pt sites far from Ru domains. Additionally, they proposed that this spillover process is kinetically limiting,

which could explain the second peak during the voltammetric oxidation of CO at high potentials. Evidently, this proposition implies that the adsorption/desorption paths of oxygen containing species at Pt sites are in a state of non-equilibrium, what was later considered unlikely (on p.356 of[77]). One possibility is that oxygen containing species are activated around CO_{ads} islands on electronically perturbed Pt domains, as we have recently assumed for the oxidation of CO on pure Pt stepped surfaces.[51]

5. Conclusions

Based on a detailed study of the CO electro-oxidation as an archetypical surface probe reaction, we unravel a number of catalytic properties underlying in Ru-modified well-ordered Pt surfaces:

i. On Ru_{step}/Pt(s)-[(*n*-1)(111)×(110)], the catalytic activity for adsorbed CO oxidation can be decoupled on that of terraces and steps. Ru at {110} Pt steps activates the reaction pathway only over the {111} terraces, and no change was detected in the catalytic activity of Pt steps free of Ru. Therefore, this means that the change in the catalytic activity of Pt sites by Ru at steps depends on the crystallographic orientation of Pt sites. Moreover, because that decoupled process of site releasing, such hierarchy allows an evaluation of the catalytic activity on terrace sites separately from that of the Pt step sites free of Ru.

ii. At both pure Pt stepped surfaces and Ru_{steps}/Pt(*hkl*), CO behaves as a motionless species during its oxidation, which implies that the bifunctional mean-field mechanism is unable to explain the catalytic enhancement in CO stripping reaction on these Ru_{steps}/Pt(*hkl*) surfaces. Electronic/strain effects seem more plausible to

explain the changes in the catalytic activity observed for (111) Pt terraces of stepped surfaces after Ru deposition on their steps.

iii. On pure Pt stepped surfaces, its catalytic activity toward CO oxidation also occurs decoupled on terraces and steps sites.

6. Associated Content

Supporting Information

Additional experimental data concerning on purely electrochemical results (cyclic voltammetries for blank and CO stripping) are presented (PDF).

Acknowledgements: M.J.S. Farias acknowledges financial support from the CNPq (Brazil), grants No. 200390/2011-2 and 313402/2013-2. G.A. Camara acknowledges financial assistance from CNPq (grants # 305494/2012-0, 309176/2015-8 and 405695/2013-6) and FUNDECT (grant # 23/200.583/2012). J.M. Feliu thanks to the MINECO (Spain) project No. CTQ2013-44083-P.

References

(1) Koper, M. T. M. *Surf. Sci.* **2004**, *548*, 1-3.

(2) Iwasita, T.; Ciapina, E. G. In *Handbook of Fuel Cells,* 1st Ed.; Wielstich, W.; Gastieger, H. A. Eds. John Wiley & Sons, Ltd, Vol. 5, 2009, p.224.

(3) Petrii, O. *J. Solid State Electrochem.* **2008**, *12*, 609-642.

(4) Kakati, N.; Maiti, J.; Lee, S. H.; Jee, S. H.; Viswanathan, B.; Yoon, Y. S. *Chem. Rev.* **2014**, *114*, 12397-12429.

(5) Bockris, J. O. M.; Wroblowa, H. *J. Electroanal. Chem. (1959)* **1964**, *7*, 428-451.

(6) Lopes, P.; Freitas, K.; Ticianelli, E. *Electrocatalysis* **2010**, *1*, 200-212.

(7) Bagotsky, V. S. In *Fundamentals of Electrochemistry*; John Wiley & Sons, Inc., 2005; pp 521-555.

(8) Petry, O. A.; Podlovchenko, B. I.; Frumkin, A. N.; Lal, H. *J. Electroanal. Chem.* **1965**, *10*, 253-269.

(9) Bagotzky, V. S.; Vassiliev, Y. B. *Electrochim. Acta* **1966**, *11*, 1439-1461.

(10) Watanabe, M.; Motoo, S. *J. Electroanal. Chem.* **1975**, *60*, 267-273.

(11) Yajima, T.; Wakabayashi, N.; Uchida, H.; Watanabe, M. *Chem. Commun.* **2003**, 828-829.

(12) Gasteiger, H. A.; Markovic, N.; Ross Jr, P. N.; Cairns, E. J. *J. Phys. Chem.* **1994**, *98*, 617-625.

(13) Liu, P.; Nørskov, J. K. *Fuel Cells* **2001**, *1*, 192-201.

(14) Lin, W. F.; Zei, M. S.; Eiswirth, M.; Ertl, G.; Iwasita, T.; Vielstich, W. *J. Phys. Chem. B* **1999**, *103*, 6968-6977.

(15) Dimakis, N.; Iddir, H.; Díaz-Morales, R. R.; Lia, R.; Bunker, G.; Chung, E. H.; Smotkin, E. S. *J. Phys. Chem. B* **2005**, *109*, 1839-1848.

(16) Kitchin, J. R.; Nørskov, J. K.; Barteau, M. A.; Chen, J. G. *Phys. Rev. Lett.* **2004**, *93*, 156801-156801-156801-156804.

(17) Mavrikakis, M.; Hammer, B.; Nørskov, J. K. *Phys. Rev. Lett.* **1998**, *81*, 2819-2822.

(18) Pinheiro, A. L. N.; Zei, M. S.; Ertl, G. *Phys. Chem. Chem. Phys.* **2005**, *7*, 1300-1309.

(19) Mueller, J. E.; Krtil, P.; Kibler, L. A.; Jacob, T. *Phys. Chem. Chem. Phys.* **2014**, *16*, 15029-15042.

(20) Zhuang, L.; Jin, J.; Abruña, H. D. *J. Am. Chem. Soc.* **2007**, *129*, 11033-11035.

(21) Mickelson, L. L.; Friesen, C. *J. Am. Chem. Soc.* **2009**, *131*, 14879-14884.

(22) Rau, M. S.; Gennero de Chialvo, M. R.; Chialvo, A. C. *J. Power Sources* **2012**, *216*, 464-470.

(23) Lu, G. Q.; Waszczuk, P.; Wieckowski, A. *J. Electroanal. Chem.* **2002**, *532*, 49-55.

(24) Davies, J. C.; Hayden, B. E.; Pegg, D. J.; Rendall, M. E. *Surf. Sci.* **2002**, *496*, 110-120.

(25) Maillard, F.; Lu, G. Q.; Wieckowski, A.; Stimming, U. *J. Phys. Chem. B* **2005**, *109*, 16230-16243.

(26) Herrero, E.; Feliu, J. M.; Wieckowski, A. *Langmuir* **1999**, *15*, 4944-4948.

(27) Crown, A.; Johnston, C.; Wieckowski, A. *Surf. Sci.* **2002**, *506*, L268-L274.

(28) Friedrich, K. A.; Geyzers, K. P.; Dickinson, A. J.; Stimming, U. *J. Electroanal. Chem.* **2002**, *524–525*, 261-272.

(29) Koper, M. T. M.; Lebedeva, N. P.; Hermse, C. G. M. *Faraday Discuss.* **2002**, *121*, 301-311.

(30) Wang, H.; Abruña, H. D. *J. Phys. Chem. Lett.* **2015**, *6*, 1899-1906.
(31) Engstfeld, A. K.; Brimaud, S.; Behm, R. J. *Angew. Chem. Int. Ed.* **2014**, *53*, 12936-12940.
(32) Engstfeld, A. K.; Klein, J.; Brimaud, S.; Behm, R. J. *Surf. Sci.* **2015**, *631*, 248-257.
(33) Chen, D.-J.; Tong, Y. J. *Angew. Chem. Int. Ed.* **2015**, *54*, 9394-9398.
(34) Camara, G. A.; De Lima, R. B.; Iwasita, T. *J. Electroanal. Chem.* **2005**, *585*, 128-131.
(35) Kibler, L. A.; El-Aziz, A. M.; Hoyer, R.; Kolb, D. M. *Angew. Chem. Int. Ed.* **2005**, *44*, 2080-2084.
(36) Baltruschat, H.; Ernst, S.; Bogolowski, N. In *Catalysis in Electrochemistry,* 1st Ed. Santos, E.; Schmickler, W., Eds. John Wiley & Sons, Inc., 2011; pp 297-337.
(37) Mello, G. A. B.; Farias, M. J. S.; Janete Giz, M.; Camara, G. A. *Electrochem. Commun.* **2014**, *48*, 160-163.
(38) Nichols, R. J.; Kolb, D. M.; Behm, R. J. *J. Electroanal. Chem.* **1991**, *313*, 109-119.
(39) Batina, N.; Will, T.; Kolb, D. M. *Faraday Discuss.* **1992**, *94*, 93-106.
(40) Massong, H.; Wang, H.; Samjeské, G.; Baltruschat, H. *Electrochim. Acta* **2000**, *46*, 701-707.
(41) Samjeské, G.; Xiao, X. Y.; Baltruschat, H. *Langmuir* **2002**, *18*, 4659-4666.
(42) Mostafa, E.; Abd-El-Latif, A.-E.-A. A.; Baltruschat, H. *ChemPhysChem* **2014**, *15*, 2029-2043.
(43) Carbonio, E. A.; Prieto, M. J.; Siervo, A. d.; Landers, R. *J. Phys. Chem. C* **2014**, *118*, 28679-28688.
(44) Clavilier, J.; Armand, D.; Sun, S. G.; Petit, M. *J. Electroanal. Chem.* **1986**, *205*, 267-277.
(45) Lang, B.; Joyner, R. W.; Somorjai, G. A. *Surf. Sci.* **1972**, *30*, 440-453.
(46) Clavilier, J.; El Achi, K.; Rodes, A. *Chem. Phys.* **1990**, *141*, 1-14.
(47) Iwasita, T.; Nart, F. C. *Prog. Surf. Sci.* **1997**, *55*, 271-340.
(48) Greenler, R. G. *J. Chem. Phys.* **1966**, *44*, 310-315.
(49) Hansen, W. N. *J. Opt. Soc. Am.* **1968**, *58*, 380-388.
(50) Climent, V.; García-Araez, N.; Herrero, E.; Feliu, J. *Russ. J. Electrochem.* **2006**, *42*, 1145-1160.
(51) Farias, M. J. S.; Camara, G. A.; Feliu, J. M. *J. Phys. Chem. C* **2015**, *119*, 20272-20282.
(52) Villegas, I.; Weaver, M. J. *J. Chem. Phys.* **1994**, *101*, 1648-1660.
(53) Persson, B. N. J.; Ryberg, R. *Phys. Rev. B* **1981**, *24*, 6954-6970.
(54) Severson, M. W.; Stuhlmann, C.; Villegas, I.; Weaver, M. J. *J. Chem. Phys.* **1995**, *103*, 9832-9843.
(55) Farias, M. J. S.; Herrero, E.; Feliu, J. M. *J. Phys. Chem. C* **2013**, *117*, 2903-2913.
(56) Farias, M. J. S.; Busó-Rogero, C.; Gisbert, R.; Herrero, E.; Feliu, J. M. *J. Phys. Chem. C* **2014**, *118*, 1925-1934.
(57) Kim, C. S.; Korzeniewski, C.; Tornquist, W. J. *J. Chem. Phys.* **1994**, *100*, 628-630.
(58) Kim, C. S.; Korzeniewski, C. *Anal. Chem.* **1997**, *69*, 2349-2353.
(59) Rodriguez, J. A.; Truong, C. M.; Goodman, D. W. *J. Chem. Phys.* **1992**, *96*, 7814-7825.

(60) Lin, W. F.; Christensen, P. A.; Hamnett, A.; Zei, M. S.; Ertl, G. *J. Phys. Chem. B* **2000**, *104*, 6642-6652.

(61) Friedrich, K. A.; Geyzers, K. P.; Linke, U.; Stimming, U.; Stumper, J. *J. Electroanal. Chem.* **1996**, *402*, 123-128.

(62) Lu, G. Q.; White, J. O.; Wieckowski, A. *Surf. Sci.* **2004**, *564*, 131-140.

(63) Lin, T. H.; Somorjai, G. A. *Surf. Sci.* **1981**, *107*, 573-585.

(64) Tränkenschuh, B.; Papp, C.; Fuhrmann, T.; Denecke, R.; Steinrück, H. P. *Surf. Sci.* **2007**, *601*, 1108-1117.

(65) Tränkenschuh, B.; Fritsche, N.; Fuhrmann, T.; Papp, C.; Zhu, J. F.; Denecke, R.; Steinrück, H. P. *J. Chem. Phys.* **2006**, *124,* 074712.

(66) Vattuone, L.; Savio, L.; Rocca, M. *Surf. Sci. Rep.* **2008**, *63*, 101-168.

(67) Smoluchowski, R. *Phys. Rev.* **1941**, *60*, 661-674.

(68) Park, J. Y.; Sacha, G. M.; Enachescu, M.; Ogletree, D. F.; Ribeiro, R. A.; Canfield, P. C.; Jenks, C. J.; Thiel, P. A.; Sáenz, J. J.; Salmeron, M. *Phys. Rev. Lett.* **2005**, *95*, 136802.

(69) Chen, Q. S.; Berna, A.; Climent, V.; Sun, S. G.; Feliu, J. M. *Phys. Chem. Chem. Phys.* **2010**, *12*, 11407-11416.

(70) Nørskov, J. K.; Bligaard, T.; Hvolbæk, B.; Abild-Pedersen, F.; Chorkendorff, I.; Christensen, C. H. *Chem. Soc. Rev.* **2008**, *37*, 2163-2171.

(71) Medford, A. J.; Vojvodic, A.; Hummelshøj, J. S.; Voss, J.; Abild-Pedersen, F.; Studt, F.; Bligaard, T.; Nilsson, A.; Nørskov, J. K. *J. Catal.* **2015**, *328*, 36-42.

(72) Morgenstern, M.; Michely, T.; Comsa, G. *Phys. Rev. Lett.* **1996**, *77*, 703-706.

(73) Picolin, A.; Busse, C.; Redinger, A.; Morgenstern, M.; Michely, T. *J. Phys. Chem. C* **2009**, *113*, 691-697.

(74) Henderson, M. A. *Surf. Sci. Rep.* **2002**, *46*, 1-308.

(75) Berná, A.; Climent, V.; Feliu, J. M. *Electrochem. Commun.* **2007**, *9*, 2789-2794.

(76) Attard, G. A.; Brew, A.; Hunter, K.; Sharman, J.; Wright, E. *Phys. Chem. Chem. Phys.* **2014**, *16*, 13689-13698.

(77) General Discussion. *Faraday Discuss.* **2002**, *121*, 331-364.

Figures

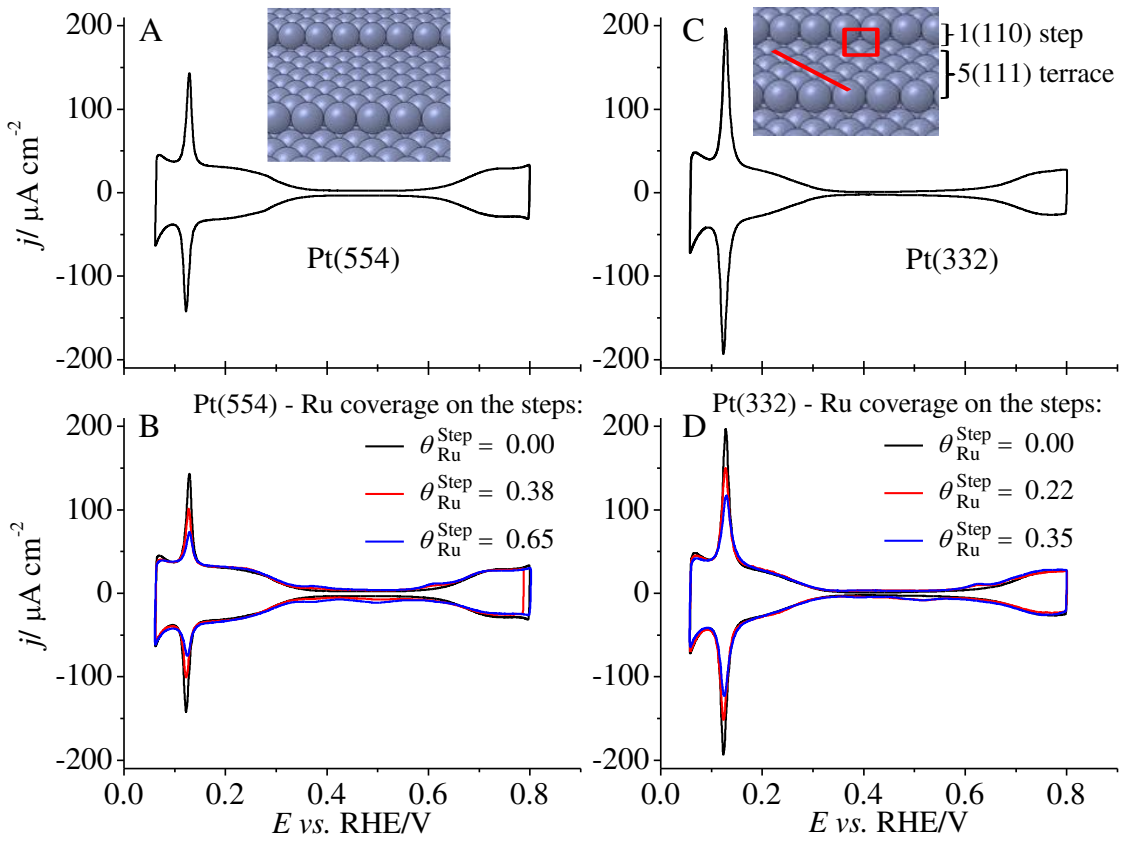

Fig. 1. Cyclic voltammetries of two stepped Pt electrodes before (A and C) and after (B and D) selective modifications of their steps by Ru. Data recorded at 0.05 V s^{-1} in 0.1 M $HClO_4$. Data includes hard sphere models of the stepped surfaces.

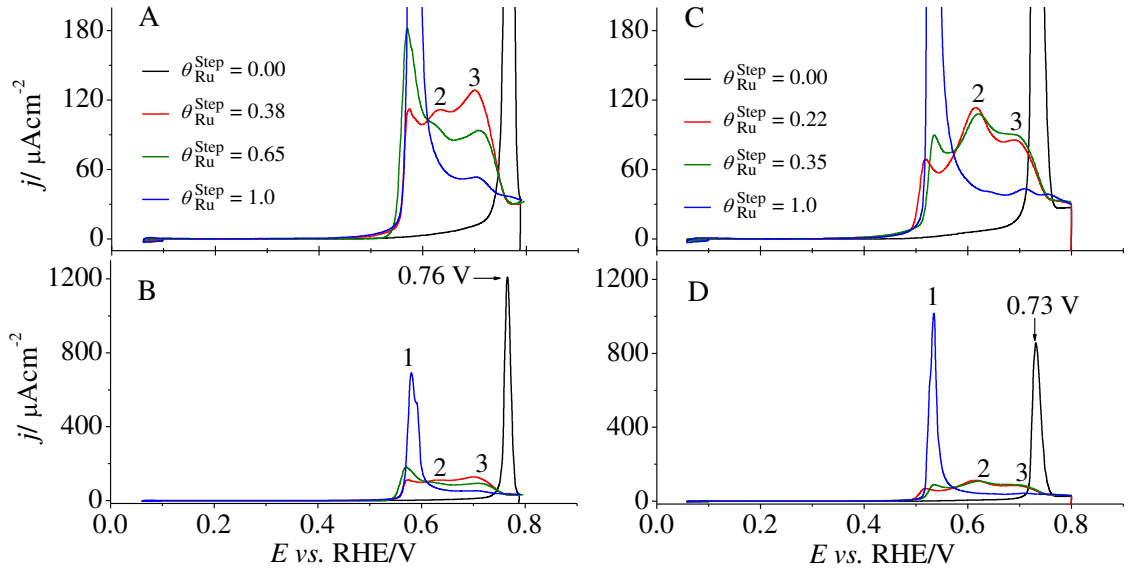

Fig. 2. CO adlayer oxidation on pure and Ru modified Pt(*hkl*) stepped electrodes: A: Pt(554); C: Pt(332). The panels B and D correspond to the panels A and C, respectively, presented on an extended scale. Data recorded at 0.05 V s^{-1} in 0.1 M $HClO_4$.

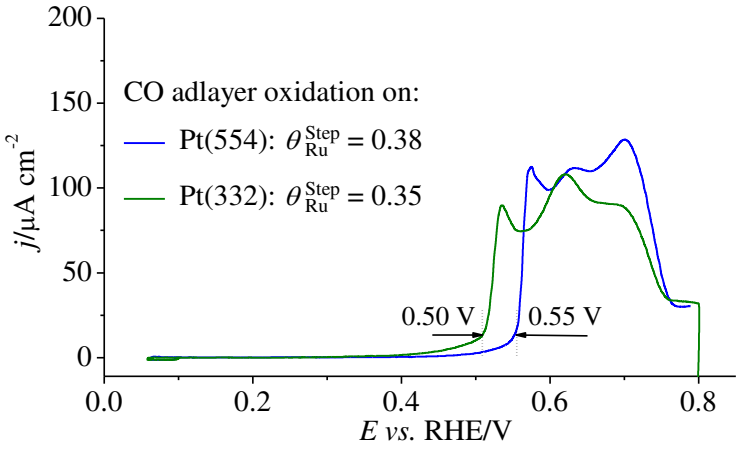

Fig. 3. Comparison between two voltammetric profiles of CO oxidation on Pt(554) and Pt(332) with their steps modified by Ru at similar coverages. Data recorded in 0.1 M $HClO_4$ at 0.05 V s^{-1}.

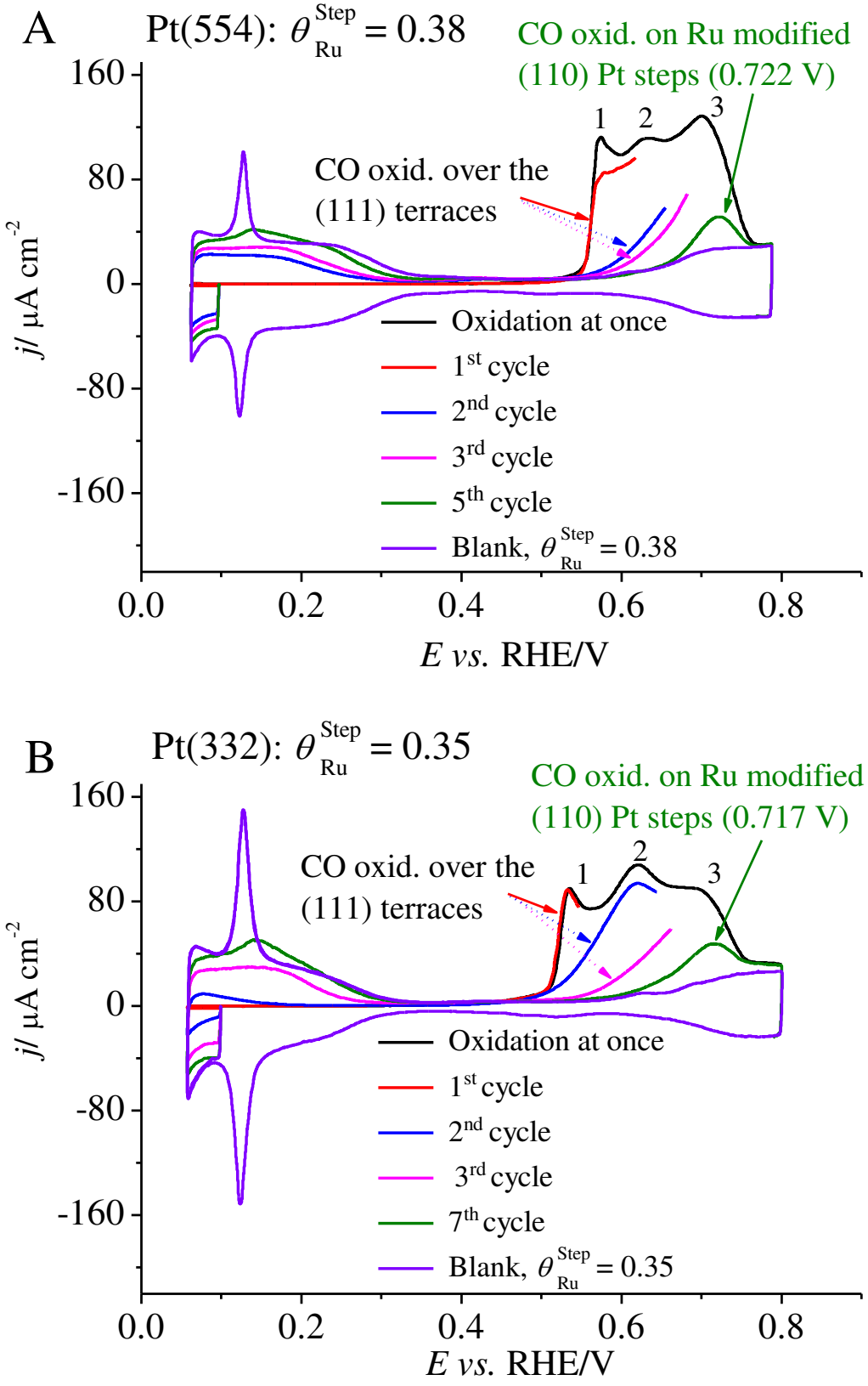

Fig. 4. Successive voltammetric cycles (indicated) collected during the oxidation of a CO adlayer on pure Pt(554) and Pt(332) and with their steps modified by Ru. Data consisted in selecting a low upper potential limit to provoke partial CO oxidations. Data recorded in 0.1 M $HClO_4$ at 0.05 V s^{-1}.

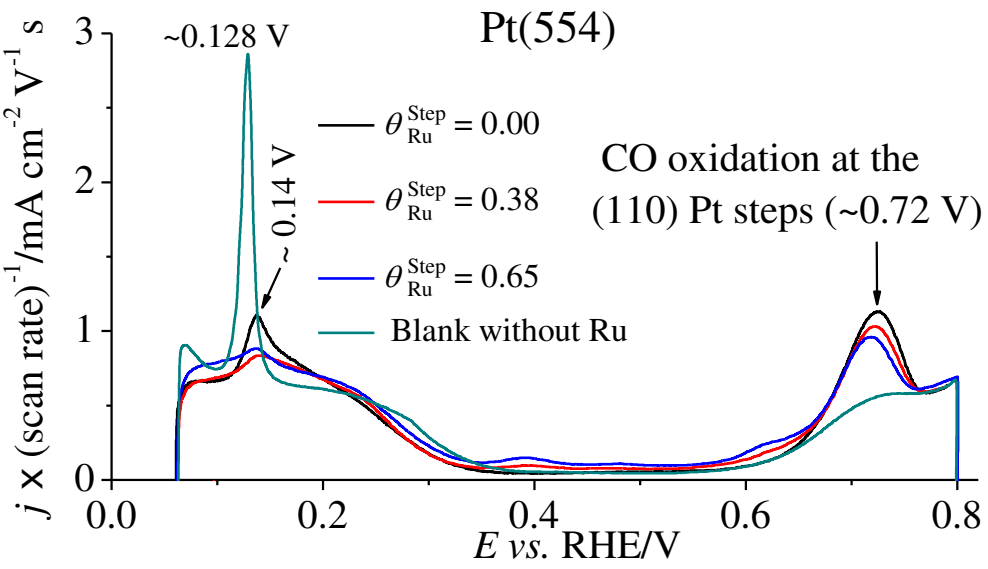

Fig. 5. Voltammetric cycles of CO oxidation on Ru-modified Pt steps (coverage indicated) and on Pure Pt(554) in 0.1 M $HClO_4$. Data recorded at 0.05 V s^{-1}.

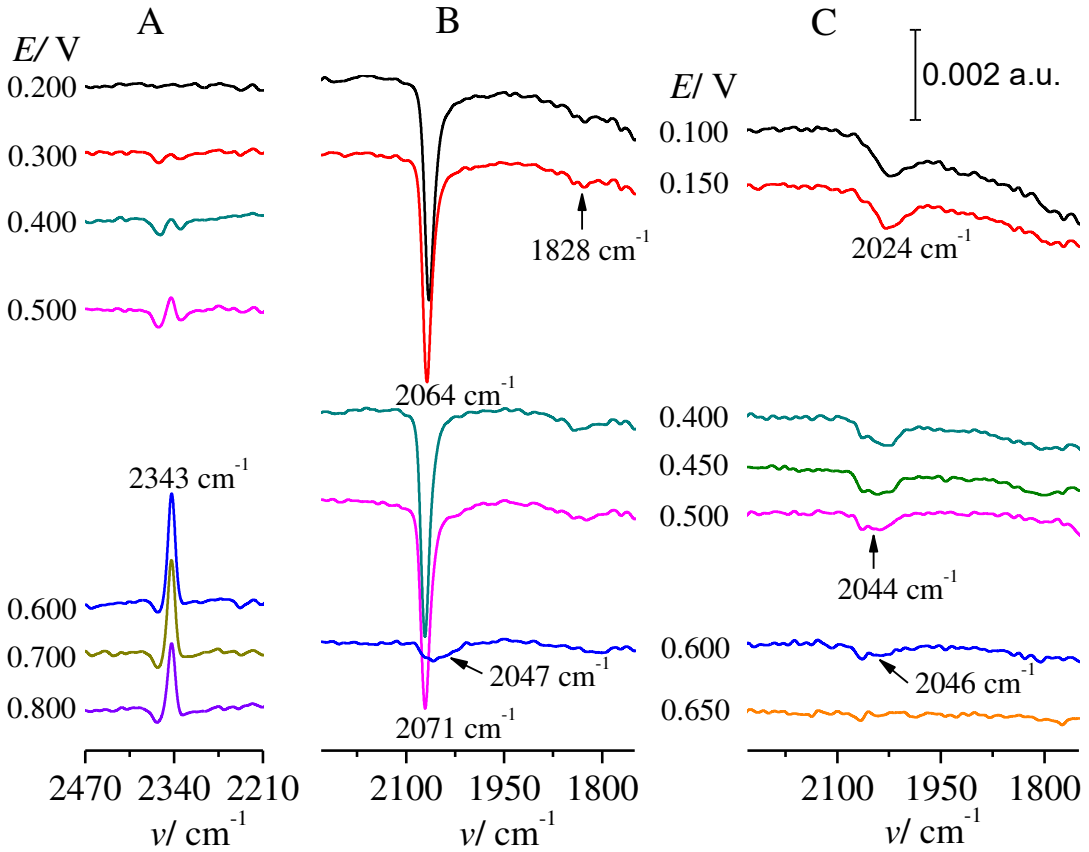

Fig. 6. *In situ* FTIR spectra of an adsorbed CO adlayer on a pure Pt(332) electrode. In panel A, the reference was collected at 0.060 V, while for the panels B and C, the reference spectra were recorded 0.800 V. Some spectra have been omitted for purposes of clarity. Data recorded in 0.1 M $HClO_4$.

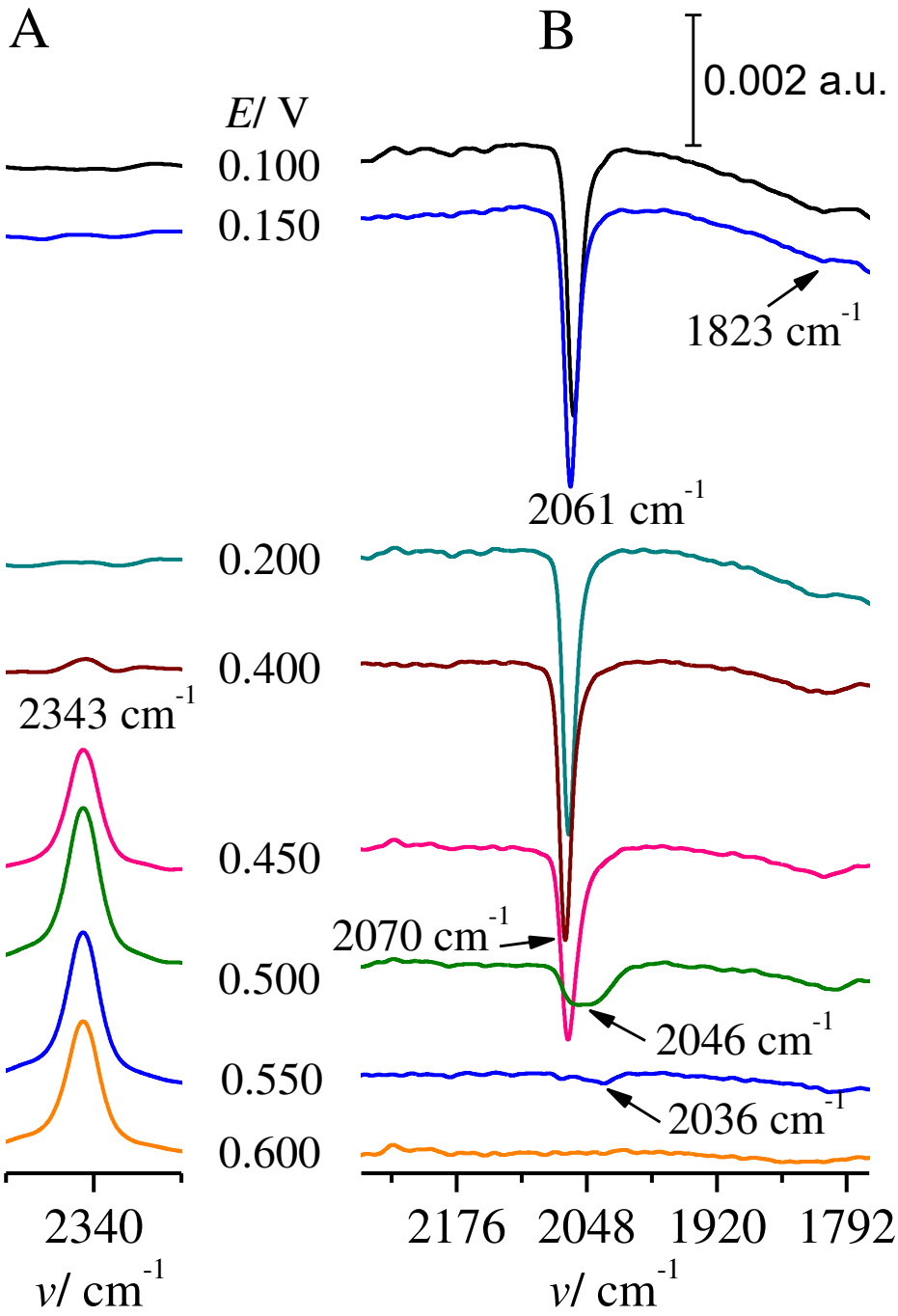

Fig. 7. *In situ* FTIR spectra of an adsorbed CO adlayer on a Ru modified Pt(332) electrode ($\theta_{\mathrm{Ru}}^{\mathrm{Step}} \simeq 0.58$). Some spectra have been omitted for clarity. In panel A, the reference spectrum was taken at 0.060 V, while in B, the reference spectrum was taken in 0.800 V. Data recorded in 0.1 M $HClO_4$.

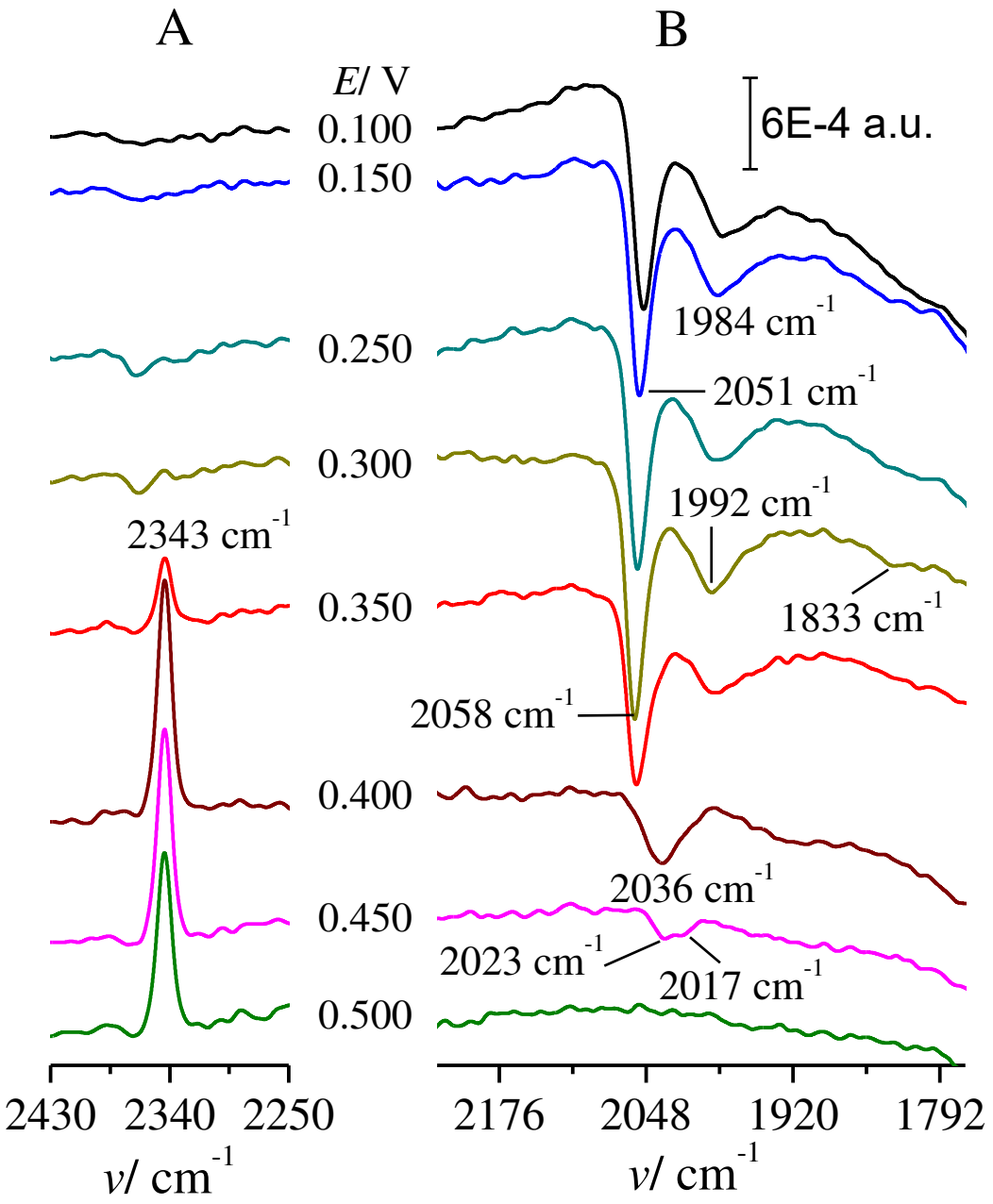

Figure 8. *In situ* FTIR spectra of an adsorbed CO adlayer on a Ru modified Pt(332) electrode (θ_{Ru}^{Step} = 1.0 plus $\theta_{Ru}^{Terrace} \simeq 0.35$). In panel A, the reference spectrum was taken at 0.060 V, while in B, the reference spectrum was taken in 0.800 V. Data recorded in 0.1 M $HClO_4$.

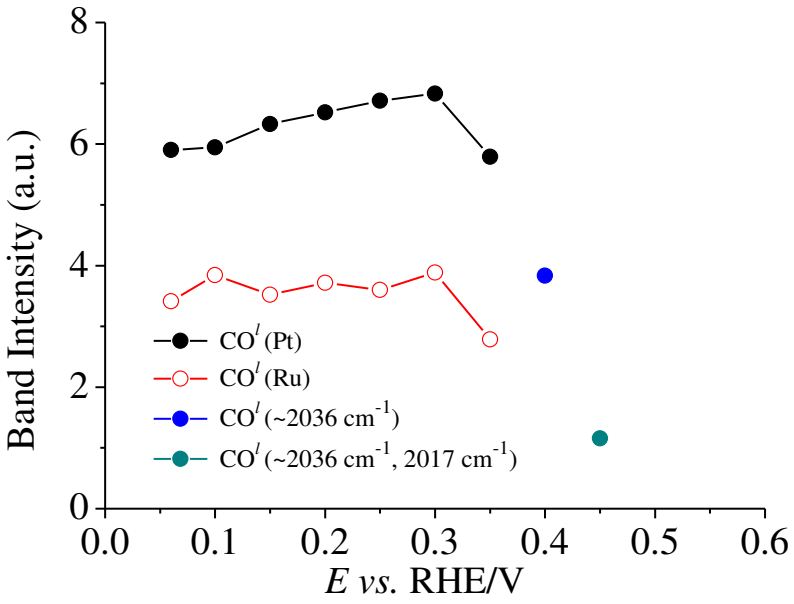

Fig. 9. Integrated band intensities for adsorbed CO on sites of Pt and Ru for a Ru modified Pt(332) electrode (θ_{Ru}^{Step} = 1.0 plus $\theta_{Ru}^{Terrace} \simeq 0.35$). Data extracted from the Figure 8.

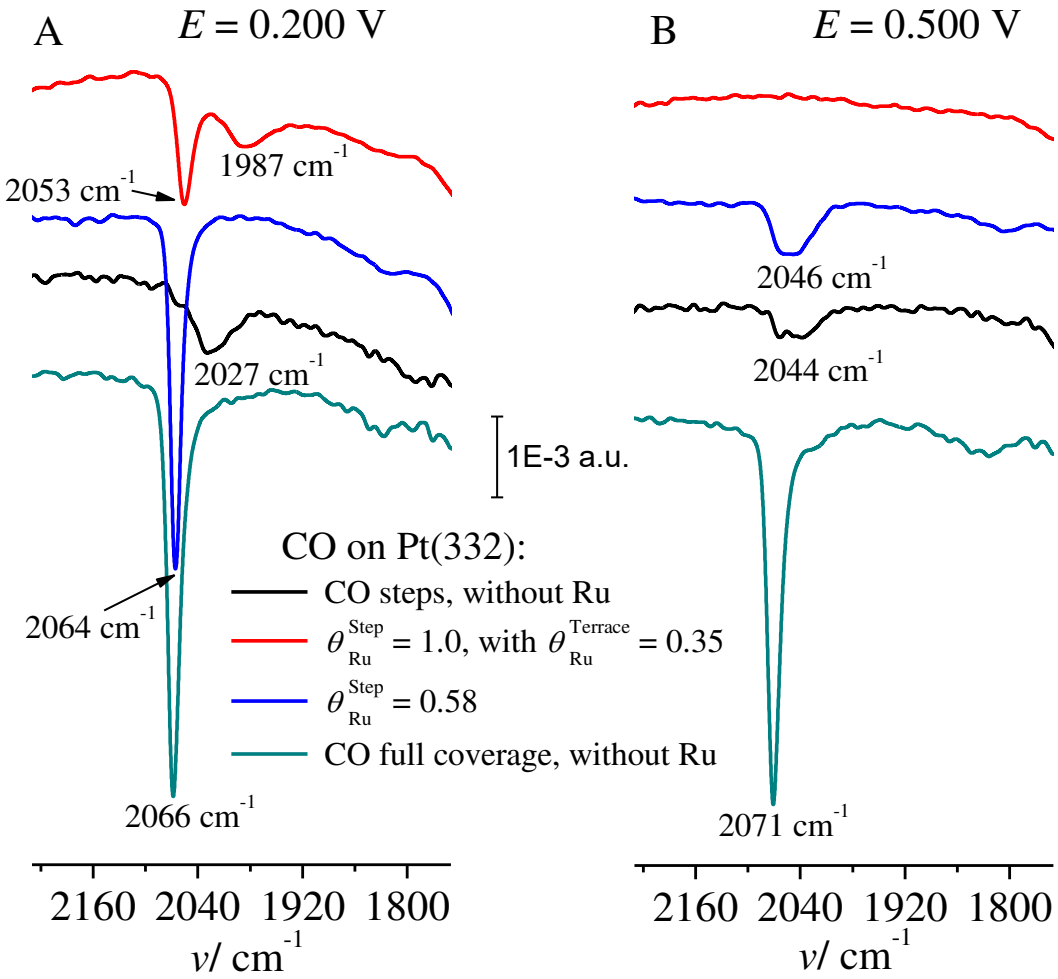

Fig. 10. *In situ* FTIR spectra of CO on pure and Ru modified Pt(332) electrode ($\theta_{Ru}^{Step} \simeq 0.58$; $\theta_{Ru}^{Step} = 1.0$ plus $\theta_{Ru}^{Terrace} \simeq 0.35$) at two electrode potentials. Reference collected at 0.800 V. For the spectra in A, the reference spectra were taken at 0.060 V, while in B, the reference spectra were taken at 0.800 V. Data recorded in 0.1 M $HClO_4$.

Graphical Abstract